Video-Capable Ultrasonic Wireless Communications Through Biological Tissues

Gizem Tabak, *Member, IEEE*, Sijung Yang, Rita J. Miller, Michael L. Oelze, *Senior Member, IEEE*, and Andrew C. Singer, *Fellow, IEEE*

***Abstract*— The use of wireless implanted medical devices (IMDs) is growing because they facilitate monitoring of patients at home and during normal activities, reduce the discomfort of patients, and reduce the likelihood of infection associated with trailing wires. Currently, radio frequency (RF) electromagnetic waves are the most commonly used method for communicating wirelessly with IMDs. However, due to the restrictions on the available bandwidth and the employable power, data rates of RF-based IMDs are limited to 267 kb/s. Considering standard definition video streaming requires data rates of 1.2 Mb/s and high definition requires 3 Mb/s, it is not possible to use the RF electromagnetic communications for high data rate communication applications such as video streaming. In this work, an alternative method that utilizes ultrasonic waves to relay information at high data rates is introduced. An advanced quadrature amplitude modulation (QAM) modem with phase-compensating, sparse decision feedback equalizer (DFE) is tailored to realize the full potential of the ultrasonic channel through biological tissues. The proposed system is tested in a variety of scenarios, including both simulations with finite impulse response (FIR) channel models, and real physical transmission experiments with *ex vivo* beef liver and pork chop samples as well as *in situ* rabbit abdomen. Consequently, the simulations demonstrated that video-capable data rates can be achieved with millimeter-sized transducers. Real physical experiments confirmed data rates of 6.7, 4.4, 4, and 3.2 Mb/s through water, *ex vivo* beef liver, *ex vivo* pork chop, and *in situ* rabbit abdomen, respectively.**

***Index Terms*— Intrabody communications, quadrature amplitude modulation (QAM) modulation, video transmission, wireless implanted medical devices (IMDs), wireless ultrasonic communications.**

I. Introduction

MANY modern wireless implanted medical devices (IMDs) make use of sensors within the body and communicate data wirelessly to a receiver or transmitter outside of the body. Because of technological advances, these devices are rapidly becoming an integral part of medical diagnostic and treatment procedures. About one in ten people in America and about 1 in 17 people living in industrialized countries rely on IMDs to regain body function, to improve life quality or to maintain survival [1]. Applications employing IMDs include, but are not limited to, pacemakers that prevent cardiovascular malfunctions, insulin monitors, and pumps that control glucose levels in the blood and adjust insulin levels accordingly, and capsule endoscopy cameras that record the digestive tract when swallowed and deliver diagnostic information about gastrointestinal conditions. Some of these devices, such as pacemakers, are designed to perform a task to overcome deficiencies of the patient's body and to be replaced invasively once their batteries are exhausted. Other devices, such as ingestible cameras, are designed to be collected after data acquisition, and the data can be processed offline. Nevertheless, these systems are not connected devices that relay high-bandwidth, real-time information. Therefore, they lack the capability of instantaneous, *in situ* intervention. They have to be followed up with invasive, interventional procedures in case an anomaly is detected, and a delay in necessary clinical intervention can result in declining patient outcomes. Hence, a medically significant need exists to develop an active and wirelessly communicating system that can relay information in real time or near real time to devices outside of the body and open up the possibility of instantaneous intervention.

Currently, radio frequency (RF) electromagnetic waves are the most frequently used method in wireless communication applications such as television, radio, or mobile phone communications. When RF waves travel through the air, they experience little attenuation. Additionally, they can operate at high frequencies, where the available bandwidth is also high. Their capability of operating at high frequencies while experiencing low loss makes RF waves appropriate for long-range, high data rate wireless communication applications through the air. However, there are various drawbacks of using RF waves with wireless IMDs to transmit data through the body. RF waves are highly attenuated in the body and have limited penetration depth. RF waves can travel 10 cm through the body from a deep-tissue IMD before experiencing 60 dB

Manuscript received May 2, 2020; accepted August 26, 2020. Date of publication September 1, 2020; date of current version February 24, 2021. This work was supported by the National Institutes of Health (NIH) under Grant R21EB025327. *(Corresponding author: Gizem Tabak.)*

The authors are with the Beckman Institute for Advanced Science and Technology, University of Illinois at Urbana–Champaign, Urbana, IL 61801 USA, and also with the Department of Electrical and Computer Engineering, University of Illinois at Urbana–Champaign, Urbana, IL 61801 USA (e-mail: tabak2@illinois.edu).

This article has supplementary downloadable material available at https://ieeexplore.ieee.org, provided by the authors.

Digital Object Identifier 10.1109/TUFFC.2020.3020776

of path loss [9]. In stark contrast, they can travel as far as 59 m through air before undergoing the same loss at the same frequency [10]. Therefore, higher power levels need to be employed to compensate for the losses in the body due to high attenuation. However, the RF signal power levels that an IMD could deploy are limited for safety reasons, as higher power increases the risk of tissue damage [11]. There are also federal regulations on the allocation of the RF spectrum use within, and outside the body. The Medical Device Radio Communications (MedRadio) guidelines impose different rules on wireless IMDs, medical body area networks (MBANs), and medical micropower networks (MMNs). While the first include the devices designed for communicating with an implant inside the body, MBAN include the network of sensors that are worn on the body, and MMN include implanted devices that help restore functions to limbs and organs. According to MedRadio guidelines, the allocated operation frequencies for the IMDs are within the range of 401–406 MHz, and the corresponding maximum allowed bandwidth is 300 kHz [12]. Moreover, MedRadio transceivers are further limited by interference regulations because they must be able to operate in the presence of primary and secondary users in those bands. Such restrictions on the transmit power and operable bandwidth lead to fundamental performance constraints for IMDs employing RF links and the data rates of the current RF-based IMDs are demonstrated to be limited to 267 kb/s [13]. Considering, for example, the standard definition video requires 1.2-Mb/s bitrate, while high-definition video streaming starts at 3 Mb/s [14], these regulations set a significant barrier against possible wireless IMD applications to include video transmission.

For many years, ultrasonic waves have been widely used as an alternative to RF electromagnetic waves in underwater communication applications, where RF waves experience significant losses. Employing ultrasonic waves for such applications enables data rates of 1.2 Mb/s over 12 m under water [15], as opposed to 50 kb/s over similar distances with electromagnetic waves [16]. Because acoustic waves have been used broadly in underwater communication applications for a long time, the characteristics of the underwater acoustic communication channel have been well established. The underwater acoustic communication channel is time varying due to motion and the changing environment, dispersive due to speed and attenuation values that vary with frequency, temperature, salinity, and pressure, frequency selective with long delay spread due to multipath, and with Doppler effects due to motion. Considering a wireless medical implant moving inside the body and communicating with a receiving probe outside of the body, most if not all of these characteristics apply to the through-body ultrasonic communication channel as well. Hence, employing advanced underwater communication techniques is a promising approach to achieve video-capable data rates through biological tissues.

The similarities between the ultrasonic communication channels through the body and under water suggest ultrasonic waves as a promising option for high data rate transmission *in situ*. Besides experiencing lower loss and hence propagating deeper in the tissue, ultrasonic waves are desirable for wireless through-body communications for several other reasons. First, because the loss is lower compared to RF electromagnetic waves, the transmission can take place at lower transmit power levels. As a result, the patient experiences lower, if not insignificant, tissue heating. Second, medical applications that utilize ultrasonic waves, such as ultrasonic imaging, have been considered as a safer option when compared with applications that utilize electromagnetic waves, such as X-ray imaging, which exposes the patients to significant amounts of ionizing radiation [17]. Third, because there are no official regulations on the ultrasonic frequency spectrum, the available bandwidth, and the corresponding potential for high data rates, are significantly higher. For all these reasons, employing ultrasonic waves for through-tissue communications at video-capable data rates offers a safe and efficient alternative to RF communications.

Ultrasonic waves have been used in the literature for wireless in-body and through-body communications, and have demonstrated the feasibility of the ultrasonic communication link through biological tissues. A comparison of recent works in the literature employing ultrasound for through-tissue communications is provided in Table I. Nevertheless, the methods in the literature either achieve lower data rates ($<$1 Mb/s) that are insufficient for standard video communication [2]–[5], [7] or achieve higher data rates with large form factor transducers ($>$1 cm) that could not be utilized in a small implantable device [6], [8], or the communication link is established through phantoms instead of real biological tissues [5], [6]. To the authors' knowledge, this work is the first work to demonstrate video-capable data rates with small form factor transducers through real *ex vivo* and *in situ* biological tissues (Fig. 1). The contributions of this work can be summarized as follows.

1) To utilize the ultrasonic through-tissue communication channel more efficiently, several underwater acoustic communication techniques are tailored to this particular application. At the transmitter end, a high order, spectrally efficient modulation technique [quadrature amplitude modulation (QAM)] is utilized to relay information at video-capable data rates. At the receiver end, a phase-tracking, sparse decision feedback equalizer (DFE) [18], [19] is used to compensate for the distortion and the intersymbol interference (ISI) introduced by the channel, and to recover the transmitted data successfully at high data rates.
2) Proposed communication system is tested with finite impulse response (FIR) channel models provided in [2]. The simulated experiments demonstrate three to ten fold increase in data rates when compared to a basic QAM modem without equalization.
3) The system is tested in a physical test platform with modular transducers that have a variety of center frequencies and sizes, and are communicating through different thicknesses of *ex vivo* beef liver slices. The experiments demonstrate that the proposed system achieves video-capable data rates with different transducers communicating through the real biological tissues.

TABLE I
COMPARISON OF RECENT WORKS EMPLOYING ULTRASOUND FOR COMMUNICATING WITH IMDS

	Transmission Medium	Transducer Size	Modulation	Equalizer	Data Rates	BER
[2]	Phantom+Scatter	2 mm	QPSK	-	200 kbps	<1e-4
[3]	Mineral oil	1.1x1.1x1.4 mm^3	QPSK (2x2 link)	-	2x125 kbps	<1e-4
[4]	Castor oil[a]	0.6x0.6x0.4 mm^3	OOK	-	95 kbps	<1e-4
[5]	Chicken phantom	1 mm	OOK/CDMA	-	1 mbps	1e-02
	Live ovine	1 mm	OOK/CDMA	-	800 kbps	1e-01
[6]	Phantom	19x44 mm^2	OFDM	Channel estimation based	28.12 mbps	1.3e-01
					12.09 mbps	1.9e-04
[7]	Kidney phantom	9.5 mm	PPM	-	70-700 kbps	<1e-6
[8]	Beef liver	19x39 mm^2	64-QAM	Adaptive equalizer	20 mbps	<1e-04
	Pork chop	19x39 mm^2	64-QAM	Adaptive equalizer	30 mbps	<1e-04

[a]Experiments are also performed with animal tissue; but the corresponding data rates are not reported.

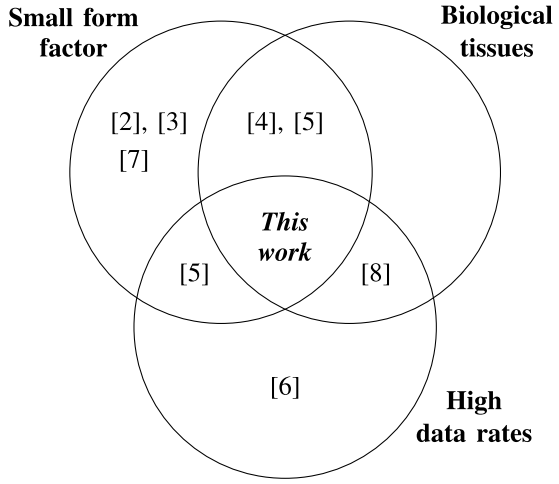

Fig. 1. This is the first work in the literature that achieves high data rates (>1 Mb/s) through real biological tissues (as opposed to phantoms) using small form factor (<1 cm) transducers.

4) The experiments are repeated with milimeter-sized, biocompatible transducers transmitting through *ex vivo* pork chops and *in situ* through the rabbit abdomen. Video-capable data rates are achieved with small form-factor transducers through these more complex transmission channels as well. Uncoded transmission yields bit error rate (BER) < 1e-3, which can be made arbitrarily low using modest forward error correction (FEC).

In an effort to elaborate on these contributions, the rest of this article proceeds as follows. Section II introduces the communication system, explains various factors that affect the data rates of the system, and proposes an advanced modem to achieve higher data rates. Section III demonstrates the capabilities of the proposed system on FIR channel models in [2]. Section IV expands the method to real physical experiments. Finally, Section V concludes the findings of this article.

II. COMMUNICATION SYSTEM

In the proposed communication system (Fig. 2), the digital data stream is obtained as video data from a camera. The video bitstream obtained from the camera is mapped into transmit symbols by the digital modulator. The symbol sequence is mixed with the carrier and shifted to passband. The passband transmit signal is then realized by an arbitrary waveform generator and transmitted through the communication channel. The communication channel is emulated in Section III with an FIR model, while in Section IV, the communication channel comprises the emitting transducer, the propagation medium (water or biological tissue), and the receiving transducer. At the receiver end, the received waveform is sampled by a digitizer. Then, the received signal is moved to baseband and aligned coarsely before channel equalization is performed to compensate for the effects of the channel and to retrieve the transmitted symbols. Finally, the retrieved symbols are mapped back to the video data to be displayed on a screen.

A. Communication Signal

In a digital communications application, the channel is usually capable of transmitting a signal waveform instead of digital bits. If the channel is band-limited as in this case, the bandwidth of this transmission waveform should match, that is lie within, the channel's available bandwidth to not lose the transmitted information. The digital modulator maps the information bits to band-limited symbols that constitute the transmission waveform so that the waveform lies within the channel band.

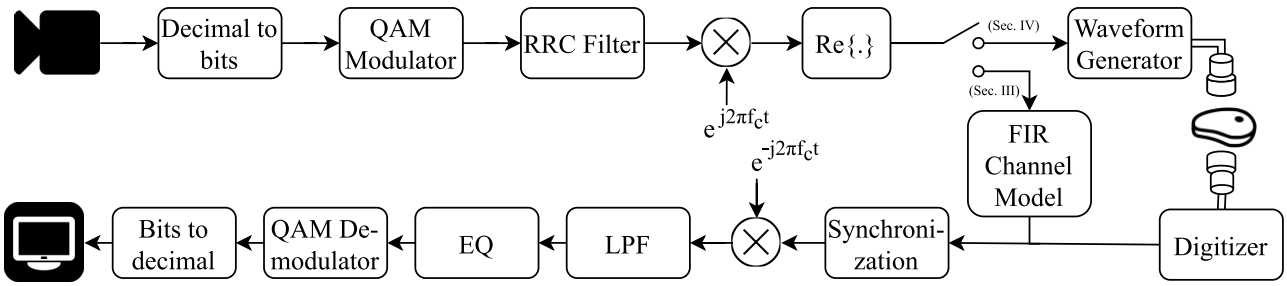

Fig. 2. Proposed communication system with equalizer (EQ) at the receiver.

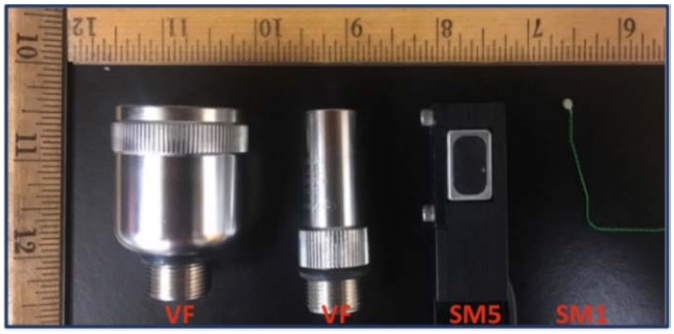

Fig. 3. Transmitting and receiving transducers with different center frequencies and form factors, with inch rulers for reference.

The data rate in a digital communication system is given by

$$R = f_b \log_2 M$$

where f_b is the symbol rate and $\log_2 M$ represents the number of bits in a symbol. f_b is limited by the bandwidth of the communication channel. Hence, to achieve high data rates, the available bandwidth should be utilized as efficiently as possible with a high-order modulation technique that can represent as many bits with one symbol as possible.

In this article, QAM is used due to its potential for high spectral efficiency. The modulator maps the binary data obtained from the webcam into N symbols $\{x_1, \ldots, x_N\} \in \{0, \ldots, M-1\}$, which corresponds to $N \log_2 M$ bits. M represents the order of QAM and indicates the number of possible complex symbol values the transmitted symbols may take. The symbols are upsampled by $L = (f_s/f_b)$, where f_s is the sampling frequency of the digital-to-analog converter in the arbitrary signal generator, and shaped with a root-raised cosine filter $p(t)$, resulting in the data packet

$$x_D(t) = \sum_{k=0}^{N-1} x_k p(t - kT_b) \tag{1}$$

where $T_b = (1/f_b)$ is the symbol period.

To detect the signal arrival at the receiver, a preamble is appended at the beginning of each data packet at the transmitter, and the preamble is matched filtered at the receiver. This synchronizing preamble can be a chirp signal, or it can be a signal waveform representing a set of symbols. In this application, linear chirp is chosen as the preamble because it is more robust to Doppler [18]. At the beginning of each data packet, a linear chirp spanning from $-(f_b/2)$ to $(f_b/2)$ followed by a guard interval is appended. The guard interval is included to prevent the spreading of the preamble into the data packet due to long channel impulse response. The transmission packet, which consists of the linear chirp preamble, guard interval, and data packet, is then mixed with a sinusoidal carrier, where f_c is the center frequency of the transmission band. The passband signal

$$x(t) = \mathcal{R}e\left\{\sum_{k=0}^{N-1} x_k p(t - kT_b) e^{j2\pi f_c t}\right\} \tag{2}$$

is then sent through the channel.

B. Communication Channel

The communication channel consists of the transmitting transducer, the transmission medium, and the receiving transducer.

1) Transducers: The physical characteristics of transducers affect the data rates and the capability of the application in different ways. In a practical deployment scenario, the transducer is limited due to size constraints and the need to be biocompatible. Furthermore, the directivity of the source affects the SNR of the received signal, and the center frequency is related to the level of attenuation of the signal and the available bandwidth.

1) *Directivity:* An essential property of a transducer is its ability to focus the transmitted energy in a particular direction and its sensitivity to the direction of the received signal. The more directional a transducer, the higher the projected and received signal power, resulting in higher SNR at the focal point. However, increased directivity requires the transmitting and receiving transducers' fields to be aligned precisely, or else the received signal might degrade significantly. Beam spread of highly directive transducers also causes substantial changes in the received signal depending on the transmitter and receiver alignment.
2) *Center Frequency:* The center frequency of a transducer, which dictates the frequency band of the passband signal, impacts the attenuation of the signal through a medium. In soft tissue at clinical ultrasonic frequencies, the attenuation increases with frequency. Therefore, higher frequencies give rise to lower signal power levels over the same transmission distance (Table II). On the

TABLE II
ATTENUATION OF ULTRASONIC WAVES AT DIFFERENT FREQUENCIES FOR DIFFERENT TISSUES [20]

		Attenuation (dB/cm)	
		1 MHz	5 MHz
Tissue	Fat	0.38	2.17
	Muscle	0.62	3.53
	Small Intestine	0.50	2.49

other hand, higher center frequency usually results in higher available bandwidth, which enables higher data rates. As an example, consider a transmission signal with 30-dB SNR at 5 cm distance in fat tissue, and assume the channel is flat within $K\%$ of the center frequency. Losses due to absorption would limit the modulation to 1024-QAM at 1 MHz, and to 64-QAM at 5 MHz, yielding data rates of 0.1 K Mb/s and 0.3 K Mb/s, respectively, for example, for $K = 10$, this corresponds to 1 Mb/s at 1 MHz and 3 Mb/s at 5 MHz. At 9 cm, same input signal would allow for 1024-QAM at 1 MHz and QPSK at 5 MHz, both yielding data rates of 0.1 K Mb/s. On the other hand, the absorption at frequencies above 9.2 MHz at 5 cm and above 5.4 MHz at 9 cm would prevent QAM communication altogether. These rough estimates, although dependent on various hypothetical assumptions such as a flat channel response, demonstrate the intricacies of the trade-off between attenuation, penetration depth, and data rate, and emphasize the importance of choosing an appropriate center frequency.

3) *Size:* The constraints imposed by the application typically limit the size of the transducer. For example, transducers that could be used in a wireless capsule endoscopy pill device would need to be smaller than the pill, which typically measures at 1.1 cm $\times$ 2.6 cm [21], whereas the size of a permanently implanted device might range from less than 1 mm^3 to a few cm^3 [22].

2) Transmission Medium: The tissue type and the different segments that constitute the tissue affect the attenuation of the signal. To explore the effects of the transmission channel on the data rates, experiments were conducted through different media such as water, *ex vivo* beef liver, *ex vivo* pork chop, and *in situ* through a rabbit abdominal wall. Beef liver and pork chop samples were initially used for this study because they are easy to obtain (e.g., can be bought from a grocery store). Furthermore, beef liver is a representative example of a homogeneous biological tissue while the pork chop is a nonhomogeneous tissue consisting of layers with different attenuation and scattering properties.

Through water and the biological tissues used in this study, different frequencies travel with small variations in speed. More importantly, they are attenuated at different rates. In addition, the layers and the inhomogeneities within the tissues, as well as their reflective surroundings, cause multipath. As a result, the channel impulse response spans some number of symbols, causing ISI. Due to ISI, the transmitted symbols spread into each other at high data rates, and they are no longer distinguishable as separate pulses at the receiver.

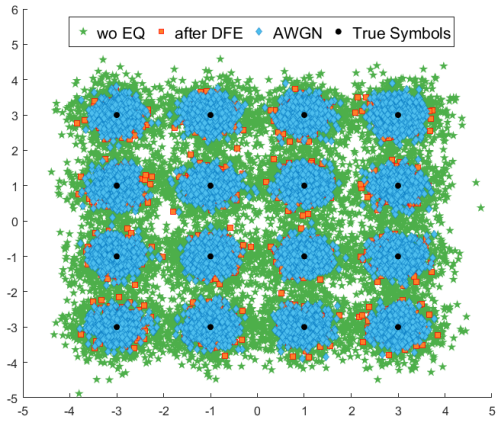

Fig. 4. Without equalization (green stars), received symbols cannot be recovered successfully at higher data rates due to spreading effects of the channel on the transmitted symbols. The equalizer compensates for most of the channel effects and the received symbols after the equalizer (orange squares) are better distinguishable. The symbols at output of the equalizer are comparable to the ones received through an AWGN channel (blue diamonds).

C. Channel Equalization

The transducers and the transmission medium impose limits on the frequency components of the signal waveform that can pass through the channel. To achieve sufficient data rates for video streaming through bandlimited communication channels, higher order modulation needs to be employed. However, because of dispersion, ISI, phase and frequency distortion, and noise, it is not possible to retrieve the higher order transmitted QAM symbols at the receiver. Moreover, due to the long impulse response of the channel, without further processing, ISI becomes a further limiting factor in the data rates of the transmission system. Without equalization, received symbols cannot be demodulated successfully at higher data rates due to degrading effects of the channel on the transmitted signal (Fig. 4). The equalizer aims to compensate these effects of the channel to achieve better BER.

There are different ways to mitigate ISI, including designing longer symbol durations, introducing guard intervals between symbols or designing a robust receiver that can compensate for the nonideal channel effects. The first two options would reduce the symbol rate, and hence the data rate. Therefore, in this work, it is most convenient to use a robust receiver that can compensate these effects of the channel and achieve better BER performance at higher data rates.

For a known channel with ISI, the optimum receiver (that minimizes sequence error probability) is a matched filter followed by a maximum likelihood sequence detector (MLSD). One disadvantage of MLSD is its complexity, which grows exponentially with the channel impulse response length. This makes MLSD an almost intractable solution for channels with relatively long delay spread. A commonly used alternative for equalization is the DFE [23], which consists of two parts:

a feedforward filter and a feedback filter. The feedforward filter operates on the received signal, and the feedback filter operates on the past symbol decisions. The operation of the feedforward filter cancels out the noncausal ISI, and the feedback filter removes causal ISI by feeding back previous symbol decisions, which are assumed to be known. When the channel impulse response is not known, the filters can be updated using a training sequence and an adaptive gradient descent [e.g., least mean squares (LMS)] or least squares [e.g., recursive least squares (RLS)] algorithm to update the filters.

A QAM signal requires coherent detection of the signal at the receiver for successful equalization and demodulation. Hence, a preamble is used to coarsely align the received signal. To obtain a reasonable coarse alignment that would fall within a few samples of the precise alignment, a preamble which has a high peak-to-sidelobe ratio in its autocorrelation function should be chosen. Furthermore, by choosing an appropriate preamble, a coarse Doppler estimate can be obtained, enabling the resampling of the signal at the receiver before demodulation and equalization. A linear chirp provides high peak-to-sidelobe ratio and it can also be used for coarse Doppler estimation [18]. After coarse alignment and Doppler correction, the remaining Doppler effects and variations during the transmission can be compensated using a phase-locked loop, which enables the receiver to adapt to the slow phase fluctuations, in combination with a fractionally spaced DFE that uses more than one received signal sample for each symbol (i.e., filter taps are located at fractions of a symbol period) to account for symbol timing drifts [18]. Once the transmitted symbols are estimated by the equalizer, they are mapped back to the bitstream and the corresponding video data.

A reverberant channel with a long impulse response may require a long feedback filter to compensate for the channel. Such equalizers may prohibit implementation in practical scenarios with limited computational resources and require excessive training data [19]. When the channel impulse response is long but sparse, a workaround would be placing zeros within the span of the feedback filter where the response does not contain significant arrivals. For the DFE proposed in this work, locations of the significant arrivals are determined with matched filtering with the linear chirp in the guard interval, and setting the feedback filter taps to zero when the matched filter output is below the threshold $\tau = 3(R_C(0)\sigma_G^2)^{1/2}$, where σ_G^2 is the noise variance estimated from the guard interval and $R_C(\tau)$ is the chirp autocorrelation function.

III. FIR Channel Simulations

To determine the theoretical limits of the QAM modem and to compare the high data rate capabilities of the proposed method and the methods in the literature, a series of simulated experiments were performed with the FIR channel measurements provided in [2]. The channel measurement data set includes impulse response models of five different types of ultrasonic communication channels through: 1) water; 2) gelatin phantom with embedded transducers, mimicking implant to implant communication inside the body (I2I-Gelatin); 3) gelatin-bone phantom with embedded transducers, mimicking implant to implant communication inside the body (I2I-Bone); 4) gelatin phantom with transducers placed on the surface of the phantom, mimicking implant to implant communication on the surface of the body (S2S-Gelatin); and 5) gelatin-bone phantom with transducers placed on the surface of the phantom, mimicking implant to implant communication on the surface of the body (S2S-Bone).

TABLE III
HIGHEST ACHIEVED DATA RATES R WITH BER $<$ 1E-4 FOR SIMULATED EXPERIMENTS WITH 80-mm FIR CHANNEL MODELS

Channel	Modulation	f_b (kHz)	R (kbps)	SNR (dB)
Water	16-QAM	625	2500	28
I2I-Gelatin	16-QAM	500	2000	23
I2I-Bone	16-QAM	625	2500	19
S2S-Gelatin	QPSK	100	200	18
S2S-Bone	QPSK	100	200	15

A. Setup

The communication system in Fig. 2 is simulated by replacing the transducers and the propagation medium with the provided channel models for 80-mm propagation distance. The transducers used in [2] are the same biocompatible 2-mm sonomicrometry crystals in this work. For each channel model, 16 experiments are repeated 100 times for each M-QAM, $M \in 2^{\{2,4,6,8\}}$, and symbol rate $f_b \in \{100, 250, 500, 625\}$ kHz. The transmit data consisted of 50 000 random bits. The bits mapped into corresponding QAM symbols and modulated on the carrier signal centered at $f_c = 1.2$ MHz. The modulated waveform was preceded with a 10-μs linear chirp and 1-ms guard interval. The simulated received signals are obtained by adding white Gaussian noise with variance that corresponds to the desired SNR, measured per bit, represented as E_b/N_o. The received signal is first matched-filtered with the linear chirp to synchronize the signal arrival time, then fed into fractionally spaced DFE, which had 18 1/2-spaced feedforward taps and 100 feedback taps. About 10% of the symbols are used for training, and DFE taps are updated with the RLS algorithm with learning rate 0.997.

B. Results

An experiment performed with an (M, f_b) pair was considered successful if it could reach BER $<$ 1e-4 for $E_b/N_o <$ 30 dB. For each channel type, successful experiments that resulted in the highest data rates by utilizing the proposed method are summarized in Table III. For each successful experiment, BER versus E_b/N_o curves in Fig. 5 were obtained by averaging the BER over 100 trials. For each trial, the received signal was also demodulated without equalization, which yields the results obtained with the basic QAM modem (QAM modulation and demodulation without equalization) in [2]. To establish the baseline for the AWGN channel, demodulation was performed on the noisy signal without channel

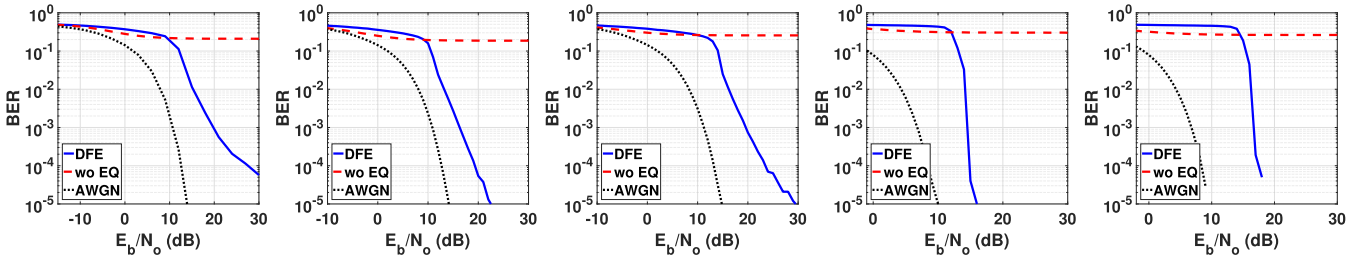

(a) Water (16-QAM, 625 kSymps) (b) I2I - Bone (16-QAM, 625 kSymps) (c) I2I - Gelatin (16-QAM, 500 kSymps) (d) S2S - Bone (QPSK, 100 kSymps) (e) S2S - Gelatin (QPSK, 100 kSymps)

Fig. 5. BER versus E_b/N_o plots of successful experiments that achieve the highest data rates using DFE for five different 80-mm channel models (blue solid line), compared with decoding without equalization (red dashed line) and AWGN channel (black dottedline). (a) Water (16-QAM, 625 kSymps). (b) I2I - Bone (16-QAM, 625 kSymps). (c) I2I - Gelatin (16-QAM, 500 kSymps). (d) S2S - Bone (QPSK, 100 kSymps). (e) S2S - Gelatin (QPSK, 100 kSymps).

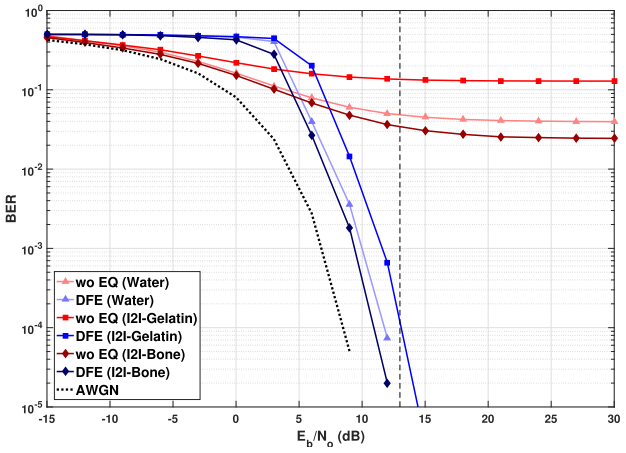

Fig. 6. With the proposed DFE modem (DFE), 1 Mb/s (QPSK, 500 kSymps) is achieved with BER of 1e-4 at 13 dB. The same communication parameters result in BER > 2e-2 with basic QAM modem (without EQ) at 13 dB.

effects. Without equalization, the channel frequency response needs to be fairly flat for successful communication with basic QAM modem to prevent interference between transmitted symbols. The channels with 2-mm transducers in [2] have a −3-dB bandwidth less than 180 kHz, which only allowed for successful communication at 400 kb/s through water, 200 kb/s through implant-to-implant channels and did not allow for successful communication with the given parameters through surface-to-surface channels without equalization. As listed in Table III, equalization enabled wider bandwidth by compensating for nonflat channel frequency response. As a result, the proposed method achieved at least 2 Mb/s, providing more than five times increase in the data rates through water and ten times increase through implant-to-implant communication channels when compared to the basic QAM modem. Moreover, it enabled communication at 200 kb/s through surface-to-surface channels, which was not possible without equalization.

The required SNR for 200 kb/s through implant-to-implant channels with a basic QAM modem is reported as 13 dB in [2]. Although SNR values required to achieve the data rates in Table III are higher than 13 dB, the proposed method achieved 1 Mb/s through water and implant-to-implant channels at 13 dB (Fig. 6). Under normal circumstances, one would expect to achieve better communication performance through water when compared to other channels in the given setup because there is less absorption and reverberation. However, the performance for the 80-mm water channel in these experiments is slightly worse than 80-mm I2I-Bone channel. This is likely due to time variations in the 80-mm water channel measurements.

In accordance with the findings in the literature, the simulations demonstrated that the basic QAM modem is not capable of communicating at high data rates required for video transmission through biological tissues with small, biocompatible transducers for given channel models. An advanced equalizer tailored for this particular application, on the other hand, shows promise toward the video-capable data rates through biological tissues at moderate to high SNR levels.

IV. Experiments

To test the capabilities of the proposed method on real data, two sets of experiments were performed on *ex vivo* and *in situ* biological tissues. In the first set of experiments, different transducers were used to communicate through water and different thicknesses of *ex vivo* beef liver to explore the capabilities of the method with transducers that have different bandwidths and received signal powers through similar type of transmission media. In the second set of experiments, small, biocompatible transducers were used through *ex vivo* pork chop and *in situ* through the rabbit abdomen to explore the capabilities of the method through different media and surrounding environments.

A. Different Transducers, Similar Channels

1) Setup: The first set of experiments were performed in a water tank filled with degassed water. In the water tank, two transducers were placed in a pitch-catch configuration. In the through-water experiments, the plastic bag, in which the beef liver was placed in further experiments, was filled with degassed water and suspended between the transducers to account for the reflective properties of the bag. In the experiments with beef liver, *ex vivo* beef livers of different thicknesses placed in between the transducers (Fig. 7). The experiments were conducted using four different transducers (Fig. 3) that have different sizes, directivities, and center

TABLE IV
EXPERIMENTAL TRANSMISSION PARAMETERS, RESULTING DATA RATES WITH BER < 1E-4 AND SNR AT THE OUTPUT OF THE EQUALIZER FOR TRANSMISSIONS THROUGH DIFFERENT MEDIA WITH DIFFERENT TRANSDUCERS

Channel Type	Transducer	Modulation Format	f_c (MHz)	f_b (MHz)	Data Rate (Mbps)	SNR (dB)
Water	VF1	64-QAM	1	1.25	7.5	22
Water	VF5	64-QAM	5	6.25	37.5	20
Water	SM1	64-QAM	1.25	1.1	**6.7**	17
Water	SM5	64-QAM	5	5	30	19
Beef Liver (2cm)	VF1	64-QAM	1	1	6	18
Beef Liver (2cm)	VF5	16-QAM	5	7.1	28.6	15
Beef Liver (2cm)	SM1	16-QAM	1.25	1.1	**4.4**	13
Beef Liver (2cm)	SM5	64-QAM	5	4.2	25	18
Beef Liver (5cm)	VF1	64-QAM	1	1	6	17
Beef Liver (5cm)	VF5	16-QAM	5	5.5	22.2	16
Beef Liver (5cm)	SM1	16-QAM	1.25	1.1	**4.4**	14
Beef Liver (5cm)	SM5	QPSK	5	5	10	11

(a) 2mm @ 1.3 MHz transducer (SM1) through 2 cm beef liver

(b) 5×8 mm^2 @ 5 MHz transducer (SM5) through 2 cm beef liver

Fig. 7. Experimental setup with different transducers suspended in a water tank, facing each other with beef liver in between. A silicone funnel was used to prevent potential paths reflecting from the tank's walls and arriving at the receiver without passing through the tissue. (a) 2 mm at 1.3-MHz transducer (SM1) through 2-cm beef liver. (b) 5 × 8 mm^2 at 5-MHz transducer (SM5) through 2-cm beef liver.

frequencies to examine the effects of each of these factors on data rates. The transducers used in the experiments were: large, focused, and directional transducers with 1- and 5-MHz center frequencies (IL0106HR and IL0506HR, Valpey Fisher, Hopkinton, MA, USA), denoted as *VF1* and *VF5*, biocompatible sonomicrometry crystals of 2-mm diameter that operate around 1.2 MHz (2-mm Round, Sonometrics, London, CAN), denoted as *SM1*, and a single-element, 5 mm × 8 mm rectangular transducer at 5 MHz (E1423, Valpey Fisher, Hopkinton, MA, USA) denoted as *SM5*. At the receiver end, because the applications are typically not limited by the transducer size outside of the body, large and highly focused transducers with 1- and 5-MHz center frequencies, *VF1* and *VF5*, were used to maximize the received signal power. The receiving transducer was also placed inside a soft, silicone funnel that would act as an acoustic damper to verify that the signal does not arrive at the receiving transducer via potential signal paths reflected from the tank's walls without traveling through the biological tissue. A direct channel was also established by connecting the signal generator to the second channel of the digitizer with a BNC cable. The delay between direct and acoustic signal arrivals corresponded to the distance between transmitting and receiving transducers, hence demonstrating successful electrical isolation and ensuring acoustic path integrity.

The transmission data were generated from random bits with different symbol rates and modulation orders as described in Section III-A. For each experiment setup, two packets of 20 000 symbols each were generated randomly with chirp and guard interval preceding each packet. In all the experiments, the signal was generated, transmitted, recorded, and then processed. An arbitrary waveform generator (PXI-5422, National Instruments, Austin, TX, USA) was used to generate the transmission signal at the preset center frequencies with different bandwidths, and coded with different modulation schemes. A digitizer was used (PXI-5124, National Instruments, Austin, TX, USA) to acquire the signal at the receiver end. To drive the National Instruments equipment and to process the received data, custom MATLAB (MathWorks, Natick, MA, USA) software was used.

At the receiver end, the signal was captured by the digitizer, coarsely aligned and corrected for Doppler effects using the chirp preamble, and the received data packet was decoded using the fractionally spaced, phase-tracking, sparse DFE [18], [19]. The equalizer had at most 53 feedforward taps and 90 feedback taps. Out of 20 000 symbols transmitted in each packet, 10% were used for training except through water with *VF5* to learn the equalizer coefficients, and the rest were used in the decision-directed mode while updating the equalizer coefficients to track the channel variations. The signal power was higher with the focused transducers, and attenuation of the signal when communicating through water was less than

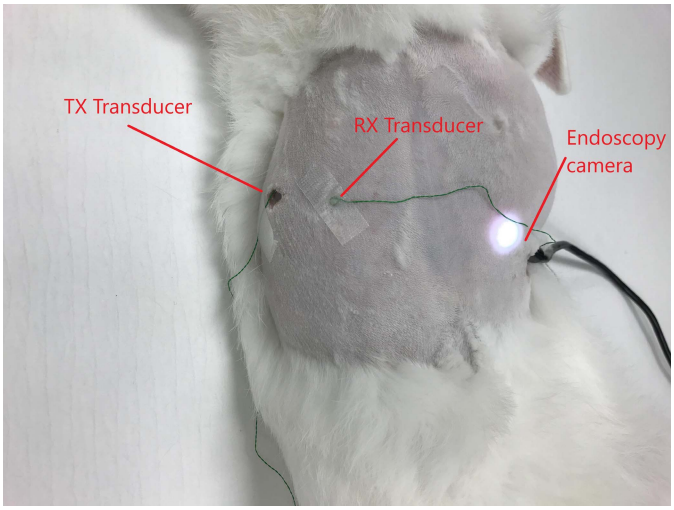

Fig. 8. Transmission of the data, obtained with an endoscopy camera, through the abdominal wall of a rabbit using 2-mm sonomicrometry crystals.

TABLE V
DATA RATES WITH CORRESPONDING BERS THROUGH DIFFERENT TISSUES USING 2-mm SM1 TRANSDUCERS

Channel Type	Data Rate	BER
Water	6.7 mbps	5e-5
Beef Liver (2 cm)	4.4 mbps	3e-5
Beef Liver (5 cm)	4.4 mbps	4e-5
Pork Chop (2 cm)	4 mbps[a]	<1e-6
Pork Chop (8 cm)	2.4 mbps[a]	<1e-3
Rabbit Abdomen	3.2 mbps	<4.2e-5

[a]Extrapolating from the output SNR

through biological tissues. These resulted in longer channel impulse responses through water with *VF1*, for which a 14% training was required for the feedback filter to cover the causal channel response. The coefficients were updated using the RLS algorithm with learning rate 0.997.

2) Results: The results of the first set of transmission experiments through water and beef liver are listed in Table IV. The thickness of the biological tissue increased attenuation, and resulted in decreased data rates for a given transmission frequency. For a given thickness, higher frequencies provided higher data rates despite the increased attenuation, thanks to higher available bandwidth. However, the form factors of the high-frequency transducers are too large to be used in an IMD such as video capsule endoscopy pill. Hence, it is more realistic to focus on the small form factor transducers (*SM1*), for which the experiments demonstrated video-capable data rates through water and beef liver.

B. Different Channels, 2-mm Transducers

1) Setup: To examine the effects of tissue properties on the data rates, the second set of experiments were performed

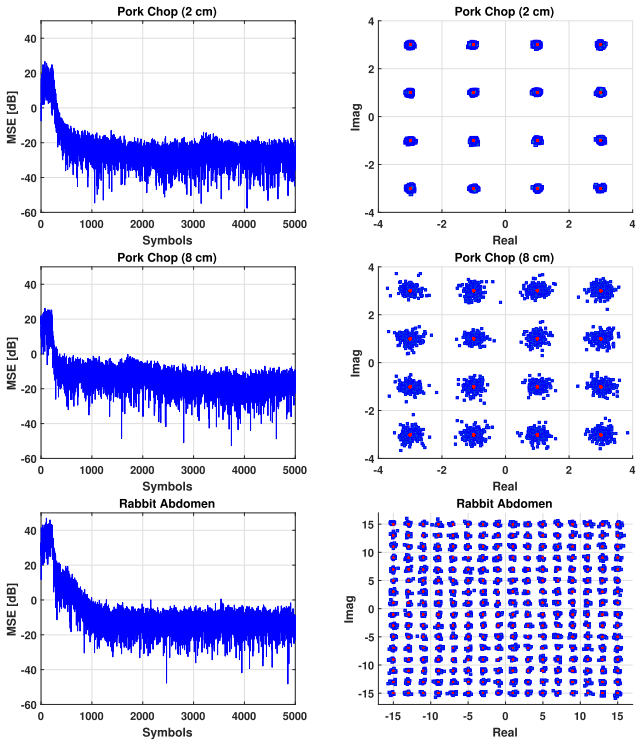

Fig. 9. Mean-squared error (left) and received signal constellation after equalization (right) for transmissions through 2-cm *ex vivo* pork chop (top), 8-cm *ex vivo* pork chop (middle), and *in situ* rabbit abdomen (bottom).

with 2-mm transducers (*SM1*) communicating through *ex vivo* pork chop and *in situ* through the rabbit abdomen. First, two *SM1* transducers were attached at each sides of 2- and 8-cm pork chops suspended in air. The transmission data were obtained from a webcam (c925e USB HD Webcam, Logitech, Lausanne, Switzerland) that has onboard h.264 video compression. Through 2- and 8-cm pork chops, 16-QAM, 1.4-MHz center frequency signal with 500-kHz symbol rate and 16-QAM, 1.4-MHz center frequency signal with 400-kHz symbol rate were transmitted, respectively.

The experiments were repeated by streaming video with SM1 transducers through the abdominal wall of a euthanized rabbit to demonstrate *in situ* transmission capabilities of the system. The transmitting transducer was implanted behind the abdominal wall, and the receiving transducer was placed on the shaved abdomen of the rabbit with gel coupling (Fig. 8). The distance between the two transducers was 2.2 cm. The data were obtained through an endoscopy camera (T01 8.5-mm USB Semi-Rigid Endoscope, Depstech) placed inside the abdomen of the rabbit. The data were sent through the rabbit abdomen with a 256-QAM, 1.1-MHz center frequency signal with 400-kHz symbol rate. A similar receiver structure to Section IV-A was used for each experiment.

2) Results: The mean-squared error plots and constellation diagrams for received, equalized symbols sent through the pork chops are displayed in the top and middle plots of Fig. 9. The results demonstrate successful demodulation of the symbols for each experiment. Although the current experimental

results achieved video-capable data rates of 2 and 1.6 Mb/s with BER < 6.25e-5, the E_b/N_o at the output of the equalizers in these experiments suggest that successful demodulation would be possible with even higher order of QAM. Specifically, 28-dB output E_b/N_o for the 2-cm pork chop experiment would allow 256-QAM, yielding data rates of at least 4 Mb/s, and the 16.4-dB output E_b/N_o for the 8-cm pork chop would allow 64-QAM, yielding 2.4 Mb/s [24].

Finally, the bottom plots in Fig. 9 display the successful transmission through the rabbit abdomen, which results in data rates of 3.2 Mb/s with BER < 4.2e-5 and output SNR of 23.4 dB. The average power consumption of the transmitting transducer was 13.5 mW at 1.2 MHz. The video transmitted through the rabbit abdomen and the corresponding decoded video can be found in the Supplementary Materials of this article.

The *ex vivo* pork chop and *in situ* rabbit experiments demonstrated that it is possible to achieve video-capable data rates through different biological tissues (Table V) using small, biocompatible transducers that could be utilized in a packaged IMD.

V. Conclusion

An online, wireless IMD that is capable of video communications or with the ability to transfer data at rates necessary for video streaming would be revolutionary in medical therapy and diagnostics. These demonstrated rates would allow the IMDs to live-stream images or download software updates, patient history, or other collected data, all within a single office visit. The regulations on and characteristics of RF electromagnetic waves restricts their use in wireless IMDs.

Previous works in the literature demonstrated the feasibility of ultrasonic waves to communicate through the body. However, the realization of such communications at high data rates with small form factor transducers were pending. In this work, it is demonstrated for the first time that achieving video-capable data rates using ultrasonic waves through different biological tissues is possible by employing refined signal processing and communication techniques. Although the phase-coherent, adaptive DFE used in this work is capable of adapting to and compensating for slow time variations in the channel, the experiments in this work were performed with *ex vivo* or *in situ* biological tissues without significant time variations in channel responses. Further work will be conducted to examine the effects of nonstationary phenomena such as breathing, blood circulation, or movements of the subjects with *in vivo* experiments.

References

[1] G. Jiang and D. D. Zhou, "Technology advances and challenges in hermetic packaging for implantable medical devices," in *Implantable Neural Prostheses 2*. Cham, Switzerland: Springer, 2009, ch. 2, pp. 27–61.

[2] T. Bos, W. Jiang, J. D'Hooge, M. Verhelst, and W. Dehaene, "Enabling ultrasound in-body communication: FIR channel models and QAM experiments," *IEEE Trans. Biomed. Circuits Syst.*, vol. 13, no. 1, pp. 135–144, Feb. 2019.

[3] M. L. Wang and A. Arbabian, "Exploiting spatial degrees of freedom for high data rate ultrasound communication with implantable devices," *Appl. Phys. Lett.*, vol. 111, no. 13, Sep. 2017, Art. no. 133503.

[4] T. C. Chang, M. L. Wang, J. Charthad, M. J. Weber, and A. Arbabian, "A 30.5 mm^3 fully packaged implantable device with duplex ultrasonic data and power links achieving 95kb/s with <10-4 BER at 8.5cm depth," in *IEEE Int. Solid-State Circuits Conf. (ISSCC) Dig. Tech. Papers*, Feb. 2017, pp. 460–461.

[5] S. H. Kondapalli, Y. Alazzawi, M. Malinowski, T. Timek, and S. Chakrabartty, "Multiaccess *in vivo* biotelemetry using sonomicrometry and M-scan ultrasound imaging," *IEEE Trans. Biomed. Eng.*, vol. 65, no. 1, pp. 149–158, Jan. 2018.

[6] E. Demirors, G. Alba, G. E. Santagati, and T. Melodia, "High data rate ultrasonic communications for wireless intra-body networks," in *Proc. IEEE Int. Symp. Local Metrop. Area Netw. (LANMAN)*, Jun. 2016, pp. 1–6.

[7] G. E. Santagati and T. Melodia, "Sonar inside your body: Prototyping ultrasonic intra-body sensor networks," in *Proc. IEEE Conf. Comput. Commun. (INFOCOM)*, Apr. 2014, pp. 2679–2687.

[8] A. Singer, M. Oelze, and A. Podkowa, "Mbps experimental acoustic through-tissue communications: MEAT-COMMS," in *Proc. IEEE 17th Int. Workshop Signal Process. Adv. Wireless Commun. (SPAWC)*, Jul. 2016, pp. 1–4.

[9] K. Sayrafian-Pour, W.-B. Yang, J. Hagedorn, J. Terrill, and K. Y. Yazdandoost, "A statistical path loss model for medical implant communication channels," in *Proc. IEEE 20th Int. Symp. Pers., Indoor Mobile Radio Commun.*, Sep. 2009, pp. 2995–2999.

[10] *IEEE Standard for Definitions of Terms for Antennas*, IEEE Standard 145-2013, 2014.

[11] FCC. *Code of Federal Regulations Title 47 Part 95 Subpart I–Medical Device Radio Communications Service*. Accessed 25 Feb. 2020. [Online]. Available: https://bit.ly/380Kyum

[12] FCC. *Radio Spectrum Allocation*. Accessed: Mar. 1, 2018. [Online]. Available: https://www.fcc.gov/engineering-technology/policy-and-rules-division/general/radio-spectrum-allocation

[13] R. Koprowski, "Overview of technical solutions and assessment of clinical usefulness of capsule endoscopy," *Biomed. Eng. OnLine*, vol. 14, no. 1, p. 111, Dec. 2015.

[14] IBM. *Multiple Bitrate Streaming With IBM Cloud Video*. Accessed: Mar. 2, 2018. [Online]. Available: https://support.video.ibm.com/hc/en-us/articles/207852127-Mutiple-bitrate-streaming-with-Ustream

[15] T. Riedl and A. Singer, "Towards a video-capable wireless underwater modem: Doppler tolerant broadband acoustic communication," in *Proc. Underwater Commun. Netw. (UComms)*, Sep. 2014, pp. 1–5.

[16] A. Palmeiro, M. Martin, I. Crowther, and M. Rhodes, "Underwater radio frequency communications," in *Proc. OCEANS IEEE Spain*, Jun. 2011, pp. 1–8.

[17] FDA. *Ultrasound Imaging*. Accessed: Mar. 2, 2018. [Online]. Available: https://www.fda.gov/Radiation-EmittingProducts/RadiationEmittingProductsandProcedures/MedicalImaging/ucm115357.htm

[18] M. Stojanovic, J. A. Catipovic, and J. G. Proakis, "Phase-coherent digital communications for underwater acoustic channels," *IEEE J. Ocean. Eng.*, vol. 19, no. 1, pp. 100–111, 1994.

[19] M. J. Lopez and A. C. Singer, "A DFE coefficient placement algorithm for sparse reverberant channels," *IEEE Trans. Commun.*, vol. 49, no. 8, pp. 1334–1338, 2001.

[20] P. Hasgall, F. Di Gennaro, C. Baumgartner, E. Neufeld, B. Lloyd, M. Gosselin, D. Payne, A. Klingenböck, and N. Kuster. (2018) *It'is Database for Thermal and Electromagnetic Parameters of Biological Tissues*. [Online]. Available: https://itis.swiss/virtual-population/

[21] Medtronic. *Pillcam SB3 System*. Accessed: Jul. 2, 2020. [Online]. Available: https://www.medtronic.com/covidien/en-us/products/capsule-endoscopy/pillcam-sb-3-system.html

[22] Y. Chen, Y.-S. Kim, B. Tillman, W.-H. Yeo, and Y. Chun, "Advances in materials for recent low-profile implantable bioelectronics," *Materials*, vol. 11, no. 4, p. 522, Mar. 2018.

[23] M. E. Austin, "Decision-feedback equalization for digital communication over dispersive channels," Res. Lab. Electron., MIT, Cambridge, MA, USA, Tech. Rep. 461, Aug. 1967.

[24] J. G. Proakis, *Digital Communications*. New York, NY, USA: McGraw-Hill, 1983.

Gizem Tabak (Member, IEEE) received the B.S. degree in electrical engineering from Bilkent University, Ankara, Turkey, in 2014, and the M.S. degree in electrical and computer engineering from the University of Illinois at Urbana–Champaign, Urbana, IL, USA, in 2016, where she is currently pursuing the Ph.D. degree.

She was a Fulbright Scholar during her M.S. studies, and a Motorola Solutions Foundations Scholar during the academic year 2019. Her research interest includes high-rate acoustic information transfer in nonideal systems.

Sijung Yang received the B.S. degree in electrical engineering from Seoul National University, Seoul, South Korea, in 2014, and the M.S. degree in electrical engineering from the University of Illinois at Urbana–Champaign, Urbana, IL, USA, in 2017, where he is currently pursuing the Ph.D. degree in electrical engineering.

His research interests are the fundamental limits and optimal implementations of seismic/acoustic/ultrasonic communication systems, and energy-efficient communication system design, which targets Internet of Things networks deployed on urban areas.

Rita J. Miller received the DVM from the University of Wisconsin, Madison, WI, USA, in 1992.

She completed a small animal medical/surgical internship at the University of Illinois at Urbana–Champaign, Urbana, IL, USA, in 1993. She joined the Bioacoustics Research Laboratory, University of Illinois at Urbana–Champaign, in 1998, where she is a Senior Research Specialist of Bioengineering. Her research interests include ultrasound emphasis, assessment of the biological effects of ultrasound on tissue, the early detection and grading of fatty liver disease, and the interaction of contrast agents with ultrasound.

Michael L. Oelze (Senior Member, IEEE) was born in Hamilton, New Zealand, in 1971. He received the B.S. degree in physics and mathematics from Harding University, Searcy, AR, USA, in 1994, and the Ph.D. degree in physics from the University of Mississippi, Oxford, MS, USA.

From 2000 to 2002, he was a Postdoctoral Researcher with Bioacoustics Research Laboratory, Department of Electrical and Computer Engineering (ECE), University of Illinois at Urbana–Champaign (UIUC), Urbana, IL, USA. From 2002 to 2004, he was an NIH Fellow conducting research in quantitative ultrasound techniques for biomedical ultrasound applications in cancer detection. In 2005, he joined the Faculty of ECE, UIUC, where he is currently a Professor and the Associate Head for Graduate Affairs. His research interests include biomedical ultrasound, quantitative ultrasound imaging for improving cancer diagnostics and monitoring therapy response, ultrasound bioeffects, ultrasound tomography techniques, ultrasound-based therapy, beamforming, and applications of coded excitation to ultrasonic imaging.

Dr. Oelze is currently a fellow of the AIUM and a member of ASA. He is a member of the Technical Program Committee of the IEEE Ultrasonics Symposium. He currently serves as an Associate Editor for the IEEE TRANSACTIONS ON ULTRASONICS, FERROELECTRICS, AND FREQUENCY CONTROL, *Ultrasonic Imaging*, and IEEE TRANSACTIONS ON BIOMEDICAL ENGINEERING.

Andrew C. Singer (Fellow, IEEE) received the S.B., S.M., and Ph.D. degrees in electrical engineering and computer science from the Massachusetts Institute of Technology (MIT), Cambridge, MA, USA, in 1990, 1992, and 1996, respectively.

Since 1998, he has been on the faculty of the Department of Electrical and Computer Engineering, University of Illinois at Urbana–Champaign, Champaign, IL, USA, where he currently holds a Fox Family Endowed Professorship with Electrical and Computer Engineering Department and serves as an Associate Dean for Innovation and Entrepreneurship with the College of Engineering. During the academic year 1996, he was a Postdoctoral Research Affiliate with the Research Laboratory of Electronics, MIT. From 1996 to 1998, he was a Research Scientist with Sanders, a Lockheed Martin Company in Manchester, U.K. He was the co-founder of Intersymbol Communications (now a subsidiary of Finisar) and OceanComm, Inc., a provider of Mb/s underwater acoustic modem technology.

Dr. Singer was elected as a fellow of the IEEE for contributions to signal processing techniques for digital communication in 2009. He was a recipient of the IEEE JOURNAL OF SOLID STATE CIRCUITS Best Paper Award in 2006 and *IEEE Signal Processing Magazine* Award in 2008. In 2014, he was named as a Distinguished Lecturer of the IEEE Signal Processing Society.